RSC Advances

ROYAL SOCIETY OF CHEMISTRY

www.rsc.org/advances

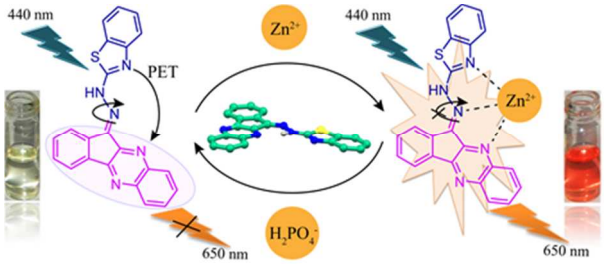

Zn^{2+} responsive (NIR) benzothiazole functionalized ninhydrin based receptor selectively sense $H_2PO_4^-$ ion.

Journal Name

RSCPublishing

ARTICLE

NIR Sensing of Zn(II) and Subsequent Dihydrogen Phosphate Detection by a Benzothiazole Functionalized Ninhydrin Based Receptor

Cite this: DOI: 10.1039/x0xx00000x

Received 00th January 2014,
Accepted 00th January 2014

DOI: 10.1039/x0xx00000x

www.rsc.org/

Abhijit Gogoi and Gopal Das

A benzothiazole functionalized ninhydrin based chemosensor ($\mathbf{L_1}$), exhibits selective naked eye detection of biologically important zinc ion (from light yellow to orange) accompanied by 'turn-on' fluorescence emission response in near infra-red (NIR) region. Most importantly, Zn^{2+} ion induced 'turn-on' fluorescence emission is also preserved in presence of Cd^{2+} and most of the other competing metal ions which clearly suggests the high sensitivity of the chemosensor towards Zn^{2+}. The job's plot suggests 1:1 binding of the $\mathbf{L_1}$ with Zn^{2+} ion with a detection limit of 6 nM. Detailed ^{1}H NMR titrations are also conducted to understand the binding behaviour of $\mathbf{L_1}$ towards the Zn^{2+} ion. The '$\mathbf{L_1}$-Zn^{2+} ensemble' further shows ratiometric response to $H_2PO_4^-$ among other competitive anions and nucleotides in the same experimental condition.

Introduction

The design and development of new fluorogenic receptors for metal ions is a promising research area in chemistry due to their essential roles in ecology, biology and clinical applications.[1] The fluorescent chemosensors are attractive because of their intrinsic high sensitivity, ease of handling, and real-time monitoring with fast response time.[2] Among the metal ions, selective and sensitive detection of Zn^{2+} ion is an intriguing task due to the similar spectroscopic properties also exhibited by the toxic Cd^{2+} ion.[3] Zn^{2+} ion is second most abundant transition metal ion in the human body after iron.[4,5] The total concentration of Zn^{2+} in mammalian cells is estimated to be in the range of 100 to 500 μM; the largest fraction is tightly bound to metallo-proteins.[6]

Again among the various features of a chemosensor, highly selective 'turn-on' emission at higher wavelength is a desirable property and mostly cited in recent years. Chemosensors which exhibit larger Stoke's shifts and emit in the near infra-red (NIR) region (650 nm – 900 nm) helps them to overcome the auto fluorescence occurring from biological samples, photo damage etc.[7] Again, the investigation of new anion sensors is an another hot research area of host-guest chemistry as the anions are ubiquitous in nature and the anionic species are of fundamental importance in many chemical, biological, medicinal, environment and industrial processes.[8] In particular among all anions, phosphate and molecules featuring this group are widely studied because of their omnipresent presence in a range of life processes. Again among them, dihydrogen phosphate plays a pivotal role in signal transduction, energy storage, and construction of the backbone of DNA and RNA.[9] However, only a few $H_2PO_4^-$ ion based receptors are known till now in literature which responds to the aforementioned anion either with enhancement or quenching of fluorescence.[10] But a ratiometric sensor is always superior from practical point of view as they are avoid of normal quenching process which occurred due to higher sensor concentration, photobleaching, microenvironment around the sensor molecule etc.[11] Various approaches utilizing hydrogen bonding, anion-π interaction, and the chelation mode of interactions have been adopted to the development of fluorescent chemosensors for pyrophosphate, phosphate ions, ATP/guanosine 5'-triphos-phate (GTP), or phosphorylated peptide.[12] Among these techniques, the metal-ligand complexes are turning out as most promising and attractive tool for anion recognition and sensing. Anions have a usual tendency for the metal–ligand complexes and their structural and geometrical flexibility can provide an excellent way of organizing anion binding groups for optimal host guest interactions. In this regard, Zn^{2+}, Cd^{2+} and Cu^{2+} complexes are extensively studied because of their normal attraction towards phosphorylated anions.[13]

In our continuing effort to design and synthesis of new sensor molecules,[14] herein we report a benzothiazole functionalized ninhydrin derived chemosensor (E)-2-(2-(11H-indeno[1,2-b]quinoxalin-11-ylidene) hydrazinyl) benzo [d]

thiazole ($\mathbf{L_1}$), which exhibits highly selective and sensitive 'turn-on' fluorescence response only to Zn^{2+} ion in longer wavelength NIR region. Zn^{2+} responsive chemosensors which show 'turn-on' fluorescence response in the NIR region are very limited.[15] Ninhydrin is known for its widespread applications in the fields of biochemical, analytical and forensic works. Again, the ninhydrin derived chemosensors exhibited beautiful colormetric response to various anions and metal ions in aqueous/ mixed aqueous solution, but there are very few references known till date.[16] The only Zn^{2+} ion induced Stoke's shift of nearly 130 nm was also maintained in physiological medium. Further the zinc-chemosensor ensemble could successfully distinguish $H_2PO_4^-$ among other competitive phosphorylated anions.

Experimental Section

General Information and Materials

All of the materials for synthesis were purchased from commercial suppliers. The absorption spectra were recorded on a Perkin-Elmer Lamda-25 UV-Vis spectrophotometer using 10 mm path length quartz cuvettes in the range 250-700 nm wavelengths, while the fluorescence measurements were carried on a Horiba Fluoromax-4 spectrofluorometer using 10 mm path length quartz cuvettes with a slit width of 5 nm at 298 K. The mass spectra of $\mathbf{L_1}$ obtained using Waters Q-ToF Premier mass spectrometer. The NMR spectra were recorded on a Varian FT-400 MHz instrument and the chemical shifts were presented in parts per million (ppm) on the scale. The following abbreviations were used to describe spin multiplicities in ^{1}H NMR spectra: s = singlet; d = doublet; t = triplet; m = multiplet. The IR spectra were recorded on a Perkin Elmer-Spectrum One FT-IR spectrometer with KBr disks in the range 4000–450 cm^{-1}.

X-Ray crystallography

The intensity data were collected using a Bruker SMART APEXII CCD diffractometer, equipped with a fine focus 1.75 kW sealed tube Mo-Kα radiation (λ = 0.71073 Å) at 298(2) K, with increasing ω (width of 0.3° per frame) at a scan speed of 3 s per frame. The SMART software was used for data acquisition. Data integration and reduction were undertaken with SAINT and XPREP[17] software. Multi-scan empirical absorption corrections were applied to the data using the program SADABS.[18] Structures were solved by direct methods using SHELXS-97 and were refined by full-matrix least squares on F2 using SHELXL-97 program package.[19] In the crystal structure, non-hydrogen atoms were refined anisotropically. Hydrogen atoms attached to all carbon atoms were geometrically fixed. Structural illustrations have been generated using ORTEP-3 and MERCURY 1.3 for Windows.[20] Crystal data, as well as details of data collection and refinement for $\mathbf{L_1}$ are summarized below.

Empirical formula : C_{22} H_{13} N_5 S, CCDC no: 1000228, Mw: 379.44, T = 298(2) K, Monoclinic, space group: P2(1)/c, a = 9.9373(12) Å, b = 13.5639(16) Å, c = 13.7420(17) Å, α = 90°, β = 102.302(6)°, γ = 90.00°, V =1809.73 $Å^3$, Z = 4, Dx (g/cm^{-3}) =1.393, m = 0.197 mm^{-1}, F(000) = 784, Reflections collected/unique = 25344/4521 [R_{int} = 0.0325], R_1 = 0.0435, wR_2 = 0.1315 [I > 2sigma(I)], R_1 = 0.0570, wR_2 = 0.1517(all data), GOF(F2) = 0.920.

Scheme 1. Synthesis of the Probes.

Results and discussion

Designing aspects of L_1

The chemosensor consists of a signalling unit (chromophore/ fluorophore) and a guest binding unit (receptor) integrated into one species through an imine bond. The benzothiazole unit thus increases the conjugation of the system and also act as good chelator for the selective binding of a metal ion. Again, the quinoxaline core also acts as chelating fluorophore. To understand the importance of the benzothiazole substituent in the sensing process, a non-chelating substituent phenyl is attached to achieve chemosensor $\mathbf{L_2}$.

Synthesis of the sensor molecules

The synthetic scheme of the probe ($\mathbf{L_1}$) and the control molecule ($\mathbf{L_2}$) are shown in scheme 1. The structure of the $\mathbf{L_1}$ is fully confirmed by NMR, mass and single crystal X-ray diffraction.

Room temperature stirring of ninhydrin (1.02 mmol) and o-phenylene diamine (1.5 mmol) in methanol with few drops of concentrated sulphuric acid for 3 hours give a flappy orange like precipitate (**L**). To a solution of **L** (1.02 mmol) in ethanol, 2-hydrazinylbenzothiazole (1.5 mmol) and few drops of concentrated sulphuric acid are added. The resulting solution is stirred for 4 hours at room temperature. It give an orange red type precipitate which then filtered and wash with ethanol and finally with water to give pure $\mathbf{L_1}$. Similarly condensation of **L** with phenyl hydrazine gives $\mathbf{L_2}$.

Important spectroscopic data for receptor $\mathbf{L_1}$: Yield = 70%; ^{1}H NMR (400 MHz, $CDCl_3$, TMS): 13.471(s, 1H), 8.250(d, 1H), 8.151(t, 2H), 7.992(d, 1H), 7.781(m, 4H), 7.568(m, 2H), 7.419(t, 1H), 7.254(d, 1H). ^{13}C: 166.872, 153.509, 151.984, 147.317, 141.952, 140.411, 138.082, 137.558, 135.077, 131.950, 131.609, 130.865, 130.395, 129.803, 129.727, 129.660, 126.297, 123.231, 122.457, 121.357, 120.742, 94.653. ESI-MS: m/z Calculated for $C_{22}H_{13}N_5S$ [M] = 379.04, found [M + H^+] = 380.1019.

Important spectroscopic data for receptor $\mathbf{L_2}$: Yield = 75 %, ^{1}H NMR (400 MHz, $CDCl_3$, TMS): 12.874(s, 1H), 8.180(d, 1H), 8.139(m, 2H), 7.795(d, 1H), 7.7541(m, 4H), 7.561(t, 2H), 7.480(t, 1H), 7.060(t, 1H), ^{13}C: 1153.212, 147.645, 143.511, 141.437, 140.583, 140.011, 132.476, 131.851, 129.921, 129.822, 129.647, 129.365, 129.304, 128.495, 122.455, 120.350, 114.173, 66.058. ESI-MS: m/z Calculated for $C_{21}H_{14}N_4$ [M] = 322.12, found [M + H$^+$] = 323.1382.

UV−Vis and Fluorescence Spectral Studies

Stock solutions of various ions (1×10^{-3} mol L^{-1}) are prepared in deionized water. Chloride or nitrate salts are used for metal ions while tetrabutyl, tetraethyl or sodium salts of the corresponding anions and nucleotides are used for the preparation of anion stock solutions. The stock solution of $\mathbf{L_1}$ and $\mathbf{L_2}$ (5×10^{-3} mol L^{-1}) are prepared in dry DMF and then diluted to 10×10^{-6} mol L^{-1} with acetonitrile. For the titration experiments, each time a 1×10^{-3} M solution of $\mathbf{L_1}$ (1×10^{-5} mol L^{-1}) in a quartz optical cell of 1 cm optical path length is titrated with the escalating concentration of stock solutions by using a micropipette. For the competitive selectivity experiment, fluorescence emission of the $\mathbf{L_1}$- Zn^{2+} ensembles are collected in the absence and presence of other competitive metal ions in an excess (50 equv.) in the aforementioned experimental medium.

Evaluation of the Apparent Binding Constant

Receptor $\mathbf{L_1}$ with an effective concentration of 10.0×10^{-6} M is used for the emission titration studies with a Zn^{2+} solution (0.2×10^{-3} M). The effective Zn^{2+} concentration is varied between 0 and 60×10^{-5} M for this titration.

Calculations for the Apparent Binding Constants Using Spectrophotometric Titration Data

The apparent binding constant for the formation of the respective complexes are evaluated using the Benesi−Hildebrand (B−H) plot (equation 1).[21]

$$1/(A-A_0) = 1/\{K(A_{max}-A_0)C\} + 1/(A_{max}-A_0) \quad (1)$$

A_0 is the absorbance of $\mathbf{L_1}$ at maximum, A is the observed absorbance at that particular wavelength in the presence of a certain concentration of the analyte (C), A_{max} is the maximum absorbance value that was obtained at λ = 536 nm during titration with varying analyte concentration, K is the apparent binding constant (M^{-1}) and was determined from the slope of the linear plot.

Finding the Detection Limit

The detection limit was calculated on the basis of the fluorescence titration. The fluorescence emission spectrum of $\mathbf{L_1}$ was measured 10 times, and the standard deviation of blank measurement was achieved. To gain the slope, the ratio of the fluorescence emission at 654 nm was plotted as a concentration of Zn^{2+}.

So the detection limit was calculated with the following equation

$$\text{Detection limit} = 3\sigma/k \quad (2)$$

where σ is the standard deviation of blank measurement, and k is the slope between the ratio of fluorescence emission versus respective analyte concentration.

Result and Discussion

Self-assembly behaviour of $\mathbf{L_1}$ in solid state

Block shaped single crystals of $\mathbf{L_1}$ were grown from slow evaporation of its propanol solution. It crystallizes in monoclinic system with P21/c space group (Z = 4). The intramolecular N2—H•••N4 (2.084A°) hydrogen bonding made the crystal to adopt a trans-amine form (C15•••N1 = 1.305Å, C16•••N2 = 1.364Å, C16•••N3 = 1.309Å) and thus forced to adopt a planer geometry. This was further helpful to decorates a number of π ••• π interactions in the packing figure.

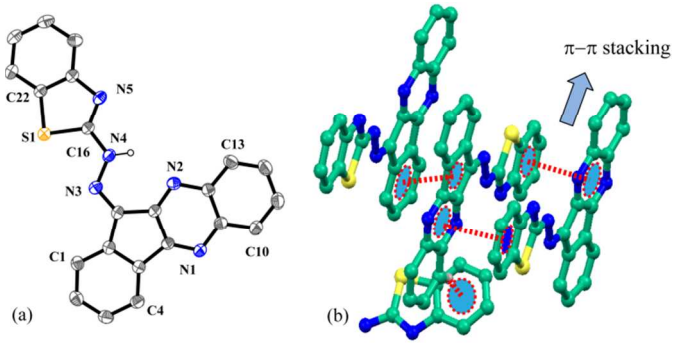

Fig. 1 (a) ORTEP presentation of $\mathbf{L_1}$ with 30% ellipsoid probability (hydrogen atoms are omitted for clarity). (b) Various non-covalent interactions in the crystal.

Each of the receptor molecule interacts with two other receptor molecules through π ••• π interactions, where the quinoxaline framework was sandwich between quinoxaline framework of one and benzothiazole functionality of the other receptor. A short C—H ••• π (2.665 Å) interaction from a third receptor molecule to the benzothiazole group extends the packing further.

Absorption based selectivity and sensitivity study with various metal ions

The sensing ability of the probe $\mathbf{L_1}$ was investigated in acetonitrile solution with various metal ions such as Zn^{2+}, Cd^{2+}, Co^{2+}, Pb^{2+}, Ni^{2+}, Cu^{2+}, Fe^{3+}, Al^{3+}, Cr^{3+}, Hg^{2+}, Ag^{+}, Mg^{2+}, Ba^{2+}, Mn^{2+}, Na^{+}, K^{+}, Ca^{2+} etc. The probe $\mathbf{L_1}$, exhibited two characteristic absorption peaks nearly at 380 nm and at 442 nm in acetonitrile solution originating from π-π* transitions and long conjugation present in the polyaromatic system. However, as evident from fig. 2a, a noticeable change in UV-Vis spectral pattern was manifested only in presence of Zn^{2+} and Cu^{2+} ions.[22] Interaction of the probe with the Zn^{2+} ion leads to emerge new absorption peaks at 536 nm and 418 nm. This was probably due to Zn^{2+} coordination induced increase in conjugation of $\mathbf{L_1}$ which in turn leads to concomitant visual colour change of the solution from light yellow to orange (Inset Fig. 2b). Further, on titration the probe solution with increasing

Zn^{2+} ion concentration showed a progressive decrease in absorbance of the characteristic 380 nm peak with concomitant increase in absorbance at 536 nm (Fig. 2b and Fig. S10). The well-defined isobestic point at 468 nm also indicates the formation of a new Zn^{2+}-$\mathbf{L_1}$ complex. Again, addition of higher equivalents of Cu^{2+} ion (10 equiv.) produces a new peak at 454 nm and a red shifted absorption maxima at 550 nm. The new isobestic points at 460 nm and 366 nm were the indicative of the formation of a new Cu^{2+}-$\mathbf{L_1}$ complex. This also leads to a visual change in colour of the solution from light yellow to light pink. More importantly, Cd^{2+} ion, the electronic congener of Zn^{2+} ion, do not produce any significant change in UV-vis pattern.

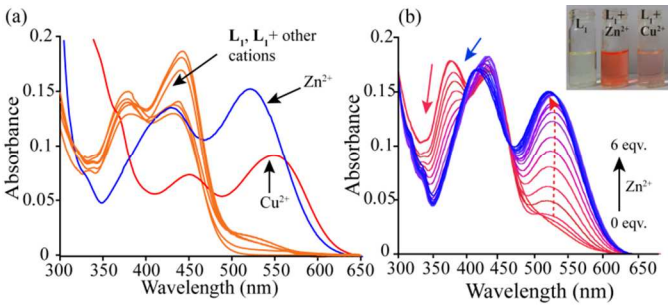

Fig. 2 Changes in absorption spectra of sensor molecule $\mathbf{L_1}$ (10μM) with the addition of (a) various guest metal ions (c = 10^{-4} M) and (b) varying concentration of Zn^{2+} ion in acetonitrile. INSET: The visual colour changes after addition of Zn^{2+} and Cu^{2+} ions to $\mathbf{L_1}$ in acetonitrile solution.

Fluorescence spectroscopic selectivity study of $\mathbf{L_1}$ with various metal ions

When excited at 440 nm, the probe $\mathbf{L_1}$ showed a distinct emission maximum at 545 nm (quantum yield <0.002) with a Stoke's shift of 103 nm in acetonitrile. In good agreement with the finding for absorption spectral studies, only Zn^{2+} ion promotes significant fluorescent enhancement to chemosensor $\mathbf{L_1}$ (Fig. 3a). Addition of Zn^{2+} ion leads to emerge a new emission maximum at 654 nm with 15.5 fold enhancement in intensity and Stoke's shift of 130 nm from a 10μM solution (Fluorescence quantum yield (Φ) = 0.11). Other metal ions, such as Cd^{2+}, Co^{2+}, Pb^{2+}, Ni^{2+}, Fe^{3+}, Al^{3+}, Cr^{3+}, Hg^{2+}, Ag^{+}, Mg^{2+}, Ba^{2+}, Mn^{2+}, Na^{+}, K^{+}, Ca^{2+} etc. caused no fluorescence change. Similarly, the coloured Cu^{2+} solution was also remain fluorescence inactive. Further, the titration spectra (Fig. 3b) of the chemosensor $\mathbf{L_1}$, with increasing Zn^{2+} ion concentration manifested a linear enhancement in intensity nearly at λ = 654 nm while the 545 nm peak was hardly got effected. A plot of fluorescent intensity as a function of Zn^{2+} ion concentration revealed that close to 20μM concentration of Zn^{2+} ion the fluorescent intensity increase sharply, and after that, the rate of enhancement was reduced (Fig 3c). Again, the linear (R^2 = 0.9902) relationship of log(FI) (fluorescence intensity) with log[Zn^{2+}] (Fig. S11) also indicates that chemosensor $\mathbf{L_1}$ can be used to determine Zn^{2+} ion concentration. And based on the fluorescence titration experiment, the calculated detection limit was 6 nM.

Rapid isomerisation around C=N and photo electron transfer (PET) from N of benzothizole to quinoxaline fluorophore are the probable cause of weak fluorescence of $\mathbf{L_1}$. While the imine N is essential for the chelation with most metal ions, to verify the importance of benzothiazole group, a control compound $\mathbf{L_2}$ was synthesized. As expected, $\mathbf{L_2}$ do not show any selectivity to any of the aforementioned cations under the same experimental condition (Fig. S12). It gives the idea of involvement of imine N, benzothiazole N/S and quinoxaline N[23] in the chelation with Zn^{2+} ion which thus cease the isomerisation process and the fluorescence increases as a result of chelation enhanced emission (CHEF) effect. Since the border line Zn^{2+} ion can interact with both hard and soft binding sites and the chemosensor $\mathbf{L_1}$ can provide required number of proper binding sites, thus it shows high selectivity for Zn^{2+} ions.

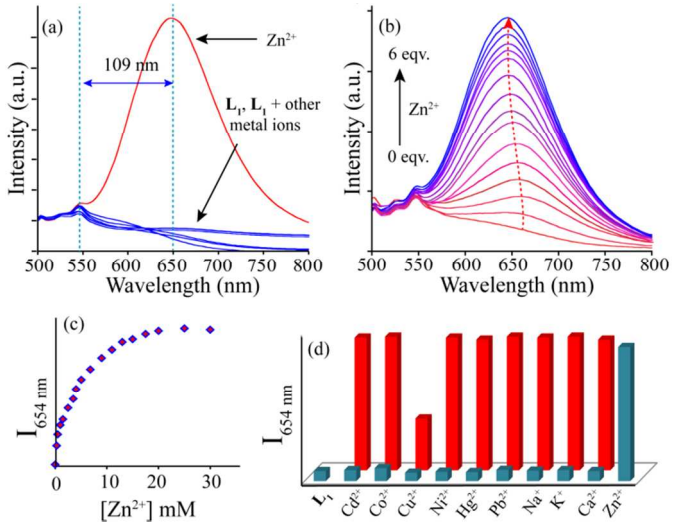

Fig. 3 Changes in fluorescence emission response of $\mathbf{L_1}$ (10μM) with (a) various metal ions (c = 10^{-4} M); (b) increasing concentration of Zn^{2+} ion in acetonitrile. (c) The I_{654} / Conc. plot showing the change in emission intensity at the λ = 654 nm with varying Zn^{2+} concentration and (d) The blue bars represents the intensity plot of $\mathbf{L_1}$ at λ = 654 nm with various metal ions while the red bars indicate the same after addition of Zn^{2+} ion to the respective $\mathbf{L_1}$ + metal ion containing solution. (λ_{ex} = 440 nm, slit width 5 nm/5 nm)

The selectivity of the chemosensor for Zn^{2+} over other competing metal ions was preserved in most of the cases (Fig. 3d). However, the switch ON red fluorescence of $\mathbf{L_1}$ with Zn^{2+} ion was interfered by the copper ion only which switches off the fluorescence probably due to its paramagnetic nature. Thus this fluorish '$\mathbf{L_1}$-Zn^{2+} ensemble' can also be used for fluorescent based sensing of Cu^{2+}. Pandey *et. al.* have used similar approach to report 'on-off-on' type sensing of Cu^{2+} and Ag^{+} ions with a fluorescent Zn(II) complex.[24] Anyway, the interference from the Cu^{2+} ion can be removed by with the addition of S^{2-} ion which restores the fluorescence based on the well-known strong affinity of S^{2-} for Cu^{2+}. However, under similar experimental condition, interaction of S^{2-} anion with 'chemosensor-Zn^{2+} ensemble' caused no change in the fluorescence output signal (Fig. S13). Again, Cu^{2+} ion would have little influence *in vivo*, as they exist at very low concentrations. Other paramagnetic metal ions like Co^{2+} and

Ni^{2+} do not affect the fluorescence emission of the 'chemosensor-Zn^{2+} ensemble'.

Considering an environmental application, the fluorescence experiment was repeated in an optimized mixed aqueous solution. The receptor could also sense the Zn^{2+} ion in presence of other interfering metal ions in an acetonitrile-buffer (HEPES) 7.4 (8:2) mixtures with nearly 6 fold enhancement in intensity (Fig. S14) at the same wavelength.

Application of the 'L_1-Zn^{2+} ensemble'

We explore the potential of this pre-synthesized $\mathbf{L_1}$-Zn^{2+} ensemble as sensor for common anionic analytes and nucleotides (Fig. 4a). This revealed that among the tested anions; F^-, Cl^-, Br^-, I^-, HSO_4^- and NO_3^- do not affect the fluorescence emissive property of the $\mathbf{L_1}$-Zn^{2+} ensemble. However, $H_2PO_4^-$ displayed an interesting concentration dependent ratiometric fluorescence response while AMP, ADP, ATP had no effect. To gain a better insight into the fluorescence behaviour, titration experiment was carried out with a fixed concentration of $\mathbf{L_1}$-Zn^{2+} ensemble and a varying amount of $H_2PO_4^-$ (Fig. 4b). The systematic variation of the amount of $H_2PO_4^-$ displayed a continuous blue shifting of the emission peak from 654 nm to 584 nm with increasing intensity. After 2.0 mole equivalents of $H_2PO_4^-$ ions, the $\mathbf{L_1}$-Zn^{2+} ensemble displayed a 22 fold enhancement in fluorescence emission intensity at 584 nm. However, addition of higher mole equivalents of the same further quenched the emission and thus a discernible colour change from orange to yellow was observed. The initial fluorescence enhancement was probably due to formation of $H_2PO_4^-$ complex with the $\mathbf{L_1}$-Zn^{2+} ensemble where the additional hydrogen bonding with the receptor might be helpful for the anion to interact with the L-M^{n+} complex. Such type of emission enhancement was also described by *Kaur et. al* with a hexaphenylbenzene derivative-Zn^{2+} ensemble.[10(d)] Further addition of $H_2PO_4^-$ anion may result in the de-complexation via initial coordination of the anion to the metal centre which was manifested by overall quenching of the fluorescence.

Further to understand more about the anion binding behaviour, we have also analyzed the changes in absorption spectra of the same $\mathbf{L_1}$-Zn^{2+} ensemble with the aforementioned anions and nucleotides. This revealed the resemblance of the spectra obtained after addition of excess $H_2PO_4^-$ anion to the $\mathbf{L_1}$-Zn^{2+} ensemble with the free $\mathbf{L_1}$ (Fig. S15). The absorption titration spectra (Fig. S16), revealed a consistent decrease in absorbance of the peak at 536 nm with concomitant increase in absorbance at 380 nm, which was the cause of the observed colour change from orange to very light yellow. Similar to the fluorescence results, other anions and nucleotides caused no change to the absorption pattern of '$\mathbf{L_1}$-Zn^{2+} ensemble'.

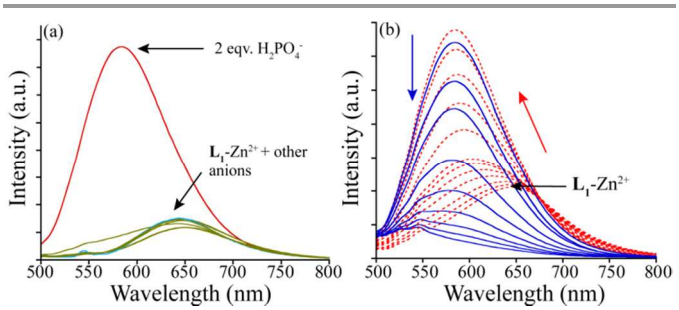

Fig. 4 Changes in fluorescence intensity of the $\mathbf{L_1}$-Zn^{2+} ensemble with (a) Various anions and nucleotides (c = 10^{-4} M) and (b) with varying concentration of $H_2PO_4^-$ anion in acetonitrile. The broken red lines refer to the change in emission upto 2 equiv. and the result of excess $H_2PO_4^-$ anion are presented by blue lines. (λ_{ex} = 440 nm, slit width 5 nm/5 nm)

Binding Mode and Composition of Metal Complex

For better understanding of the sensing mechanism and the resulting metal ion–sensor complex, Job's plot and ^{1}H NMR titration were carried out. The apparent binding constant (K) for the formation of $\mathbf{L_1}$–Zn^{2+} complex was calculated by using B–H method from the absorption titration spectra. A 1:1 binding stoichiometry was suggested by the job's plot on the basis of change in absorbance at 536 nm and the apparent binding constant value was found to be 8×10^4 M^{-1} (Fig. S17).

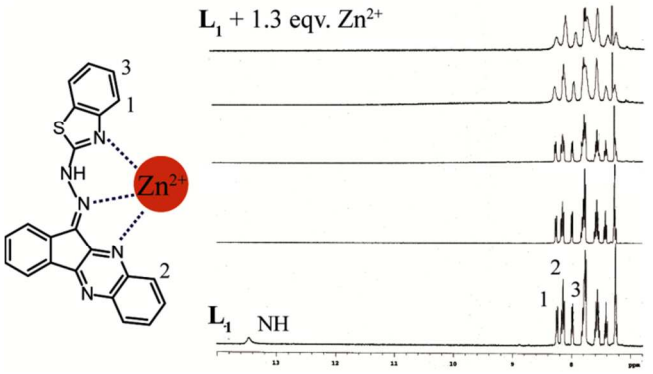

Fig. 5 ^{1}H NMR stack plot of $\mathbf{L_1}$ with increasing concentration of Zn^{2+} ion in $CDCl_3$ at room temperature with the probable binding mode.

However, due to the poor solubility of the sensor molecule in CD_3CN, the NMR titration was carried out in $CDCl_3$ solution. It showed a singlet in the very downfield region of the spectra which might be the NH proton of the benzothiazole unit due to the conjugation in the system. However, addition of Zn^{2+} ion causes disappearance of this signal (Fig. 5). A close inspection in the titration stack plot also revealed that the CH(1) proton undergoes a downfield shift from 8.250 ppm to 8.286 ppm upon addition of 1 equivalent of Zn^{2+} ion, while CH(2) proton shifted upfield from 8.151 to 8.132 and CH(3) proton shifted from 7.991 ppm to 7.961 ppm. Negligible changes were observed for the rest of the protons which means that these CHs were not bound to zinc ion. Based on these a plausible binding scheme is also represented in fig. 5, where the nitrogen atoms of benzothiazole, quinoxaline and hydrazide functionalities are the most probable chelating atoms.

Conclusion

In conclusion, we have synthesized a novel benzothiazole functionalized ninhydrin based chemosensor $\mathbf{L_1}$, which impels excellent colorimetric and 'turn-on' fluorometric response in near infra-red region (NIR) only towards Zn^{2+} ion. These spectral changes are significant enough to enable naked eye detection of Zn^{2+} ion in physiological medium also. Most importantly, the sensitivity of $\mathbf{L_1}$ for Zn^{2+} ion was also preserved in presence of its congener Cd^{2+} and most of the other tested metal ions even when present in excess. The job's plot from the titration data suggests a 1:1 ($\mathbf{L_1}$: Zn^{2+}) binding stoichiometry and the calculated detection limit was 6 nM. Nature of the Zn^{2+} binding mode with $\mathbf{L_1}$ was also analysed with ^1H NMR titration. Finally, $\mathbf{L_1}$-Zn^{2+} ensemble could selectivity sense and differentiate $H_2PO_4^-$ from pyrophosphate, ATP, ADP etc. nucleotides and other common anions.

Acknowledgements

G.D. acknowledges CSIR (01/2727/13/EMR-II) and Science & Engineering Research Board (SR/S1/OC-62/2011) New Delhi, India for financial support, CIF IITG for providing instrument facilities. AG acknowledges IIT Guwahati for fellowship.

Notes and references

Department of Chemistry, Indian Institute of Technology Guwahati, Guwahati 781039, India, Fax: + 91 361 2582349; Tel: +91 3612582313

1 E. L. Que, D. W. Domailli and C. J. Chang, *Chem. Rev*., 2008, **108**, 1517-1549.

2 (a) R. M. Manez and F. Sancenon, *Chem. Rev*., 2003, **103**, 4419-4476; (b) J. S. Kim and D. T. Quang, *Chem. Rev*., 2007, **107**, 3780-3799.

3 M. Waisberg, P. Joseph, B. Hale and D. Beyersmann, *Toxicology*, 2003, **192**, 95-117.

4 C. J. Frederickson, J. Y. Koh, A. I. Bush, *Nat. Rev. Neurosci*., 2005, **6**, 449-462.

5 (a) J. M. Berg and Y. Shi, *Science*, 1996, **271**, 1081-1085; (b) B. L. Vallee and D. S. Auld, *Biochemistry*, 1990, **29**, 5647-5659.

6 (a) C. J. Frederickson, *Int. Rev. Neurobiol*., 1989, **31**, 145-238; (b) C. J. Frederickson, S. W. Suh, J.-Y. Koh, Y. K. Cha, R. B. Thompson, C. J. LaBuda, R. V. Balaji and M. P. Cuajungco, *J. Histochem. Cytochem*., 2002, **50**, 1659-1662; (c) G. Danscher and M. Stoltenberg, *J. Histochem. Cytochem.,* 2005, **53**, 141-153; (d) C. J. Chang, J. Jaworski, E. M. Nolan, M. Sheng and S. J. Lippard, *Proc. Natl. Acad. Sci.,* U.S.A. 2004, **101**, 1129-1134; (e) P. D. Zalewski, S. H. Millard, I. J. Forbes, O. Kapaniris, A. Slavotinek, W. H. Betts, A. D. Ward, S. F. Lincoln and I. Mahadevan, *J. Histochem. Cytochem*., 1994, **42**, 877-884; (f) B. Lukowiak, B. Vandewalle, R. Riachy, J. -K. Conte, V. Gmyr, S. Belaich, J. Lefebvre and F. Pattou, *J. Histochem. Cytochem*., 2001, **49**, 519-528.

7 (a) Z. Guo, W. Zhu, M. Zhu, X. Wu and H. Tian, *Chem.-Eur. J.*, 2010, **16**, 14424-14432; (b) X. Peng, T. Wu, J. Fan, J. Wang, S. Zhang, F. Song and S. Sun, *Angew. Chem. Int. Ed.*, 2011, **50**, 4180-4183.

8 (a) R. M. Duke, E. B. Veale, F. M. Pfeffer, P. E. Kruger and T. Gunnlaugsson, *Chem. Soc. Rev*., 2010, **39**, 3936-3953; (b) J. L. Sessler, P. A. Gale and W. -S. Cho, RSC Publishing, Cambridge, UK, 2006.

9 W. Saenger, Principles of Nucleic Acid Structure, Springer, New York, 1988.

10 (a) A. Rostami, C. J. Wei, G. Gue´rin and M. S. Taylor, *Angew. Chem. Int. Ed*., 2011, **50**, 2059-2062; (b) C. Gao, G. Gao, J. Lan and J. You, *Chem. Commun.,* 2014, **50**, 5623-5625; (c) M. Alfonso, A. Espinosa, A. Tarraga and P. Molina, *Org. Lett*., 2011, **13**, 2078-2081; (d) V. Bhalla, V. Vij, M. Kumar, P. R. Sharma and T. Kaur, *Org. Lett*., 2012, **14**, 1012-1015; (e) J. Wang and C. -S. Ha, *Analyst*, 2010, **135**, 1214-1218; (f) X. –L. Ni, X. Zeng, C. Redshaw and T. Yamato, *J. Org. Chem*., 2011, **76**, 5696-5702.

11 (a) S. Das, S. Karmakar, S. Mardanya and S. Baitalik, *Dalton Trans*., 2014, **43**, 3767-3782; (b) Z. Liu, C. Zhang, X. Wang, W. He and Z. Guo, *Org. Lett*., 2012, **14**, 4378-4381; (c) W. -C. Lin, S. -K. Fang, J. -W. Hu, H. -Y. Tsai and K. -Y. Chen, *Anal. Chem*., 2014, **86**, 4648-4652.

12 (a) G. Sánchez, D. Curiel, W. Tatkiewcz, I. Ratera, A. Tárraga, J. Veciana and P. Molina, *Chem. Sci*., 2014, **5**, 2328-2335; (b) Y. Sun, C. Zhong, R. Gong and E. Fu, *Org. Biomol. Chem*., 2008, **6**, 3044-3047; (c) K. Ghosh, A. R. Sarkar, A. Samadder and A. R. K. Bukhs, *Org. Lett.*, 2012, **14**, 4314-4317; (d) J. -H. Liao, C. -T. Chen and J. -M. Fang, *Org. Lett*., 2002, **4**, 561-564; (e) Z. Xu, N. J. Singh, J. Lim, J. Pan, H. N. Kim, S. Park, K. S. Kim and J. Yoon, *J. Am. Chem. Soc*., 2009, **131**, 15528-15533; (f) H. Jeon, S. Lee, Y. Li, S. Park and J. Yoon, *J. Mater. Chem.*, 2012, **22**, 3795-3799; (g) N. Ahmed, B. Shirinfar, I. Geronimo and K. S. Kim, *Org. Lett*., 2011, **13**, 5476-5479.

13 (a) O. G. Tsay, S. T. Manjare, H. Kim, K. M. Lee, Y. S. Lee and D. G. Churchill, *Inorg. Chem*., 2013, **52**, 10052-10061; (b) M. Strianese, S. Milione, A. Maranzana, A. Grassia and C. Pellecchiaa, *Chem. Commun*., 2012, **48**, 11419-11421; (c) Y. Kurishita, T. Kohira, A. Ojida and I. Hamachi, J. *Am. Chem. Soc*., 2012, **134**, 18779-18789; (d) W. -H. Chen, Y. Xing and Y. A Pang, *Org. Lett*., 2011, **13** 1362-1365; (e) B. B. Shi, Y. M. Zhang, T. B. Wei, P. Zhang, Q. Lin and H. Yao, *New J. Chem*., 2013, **37**, 3737-3744; (f) M. J. Kim, K. M. K. Swamy, K. M. Lee, A. R. Jagdale, Y. Kim, S.-J. Kim, K. H. Yoo and J. Yoon, *Chem. Commun*., 2009, 7215-7217; (g) W. Zhu, X. Huang, Z. Guo, X. Wu, H. Yu and H. Tian, *Chem. Commun.*, 2012, **48**, 1784-1786; (h) X. Feng, Y. An, Z. Yao, C. Li and G. Shi, *ACS Appl. Mater. Interfaces*, 2012, **4**, 614-618.

14 (a) C. Kar, M. D. Adhikari, A. Ramesh and G. Das, *Inorg. Chem.,* 2013, **52**, 743-752; (b) B. K. Datta, S. Mukherjee, C. Kar, A. Ramesh and G. Das, *Anal. Chem*., 2013, **85**, 8369-8375.

15 (a) J. Cao, C. Zhao, X. Wang, Y. Zhanga and W. Zhu, Chem. Commun., 2012, **48**, 9897–9899; (b) J. Wang, Y. Li, E. Duah, S. Paruchuri, D. Zhou and Y. Pang, J. Mater. Chem. B, 2014, **2**, 2008-2012.

16 (a) A. Kumar, V. Kumar and K. K. Upadhyay, *Tetrahedron Lett.*, 2011**, 52,** 6809–6813; (b) A. Kumar, V. Kumar, U. Diwan and K. K. Upadhyay, *Sens. Actuators B*., 2013, **176**, 420-427.

17 Saint, Smart and XPREP, Siemens Analytical X-ray Instruments Inc., Madison, Wisconsin, USA, 1995.

18 G. M. Sheldrick, SADABS: software for Empirical Absorption Correction, University of Gottingen, Institute fur Anorganische Chemieder Universitat, Tammanstrasse 4, D-3400 Gottingen, Germany, 1999–2003.

19 G. M. Sheldrick, SHELXS-97, University of Gottingen, Germany, 1997; G. M. Sheldrick, SHELXL-97, Program for Crystal Structure Refinement; University of Gottingen, Germany, 1997.

20 L. J, Farrugia, ORTEP-3 for Windows - a version of ORTEP-III with a Graphical User Interface (GUI) *J. Appl. Crystallogr*., 1997, **30**, 565; Mercury 1.3 Supplied with Cambridge Structural Database, CCDC: Cambridge, U.K., 2003–2004.

21 (a) H. A. Benesi and J. H. Hildebrand, *J. Am. Chem. Soc*., 1949, **71**, 2703-2707; (b) F. Han, Y. Bao, Z. Yang, T. M. Fyles, J. Zhao, X. Peng, J. Fan, Y. Wu and S. Sun, *Chem.-Eur. J*., 2007, **13**, 2880-2892.

22 S. Anbu, R. Ravishankaran, M. F. C. G. Silva, A. A. Karande and A. J. L. Pombeiro; *Inorg. Chem*., 2014, **53**, 6655–6664.

23 M. Alfonso, A. Tárraga, P. Molina, *J. Org. Chem*., 2011, **76**, 939-947.

24 R. Pandey, P. Kumar, A. K. Singh, M. Shahid, P.-Z. Li, S. K. Singh, Q. Xu, A. Misra and D. S. Pandey, *Inorg. Chem*., 2011, **50**, 3189–3197.